

ARTICLES

A new progeroid syndrome reveals that genotoxic stress suppresses the somatotroph axis

Laura J. Niedernhofer^{1,4}, George A. Garinis¹, Anja Raams¹, Astrid S. Lalai¹, Andria Rasile Robinson⁴, Esther Appeldoorn¹, Hanny Odijk¹, Roos Oostendorp¹, Anwaar Ahmad⁴, Wibeke van Leeuwen², Arjan F. Theil¹, Wim Vermeulen¹, Gijsbertus T. J. van der Horst¹, Peter Meinecke⁵, Wim J. Kleijer³, Jan Vijg⁶, Nicolaas G. J. Jaspers¹ & Jan H. J. Hoeijmakers¹

XPF-ERCC1 endonuclease is required for repair of helix-distorting DNA lesions and cytotoxic DNA interstrand crosslinks. Mild mutations in *XPF* cause the cancer-prone syndrome xeroderma pigmentosum. A patient presented with a severe *XPF* mutation leading to profound crosslink sensitivity and dramatic progeroid symptoms. It is not known how unrepaired DNA damage accelerates ageing or its relevance to natural ageing. Here we show a highly significant correlation between the liver transcriptome of old mice and a mouse model of this progeroid syndrome. Expression data from *XPF-ERCC1*-deficient mice indicate increased cell death and anti-oxidant defences, a shift towards anabolism and reduced growth hormone/insulin-like growth factor 1 (IGF1) signalling, a known regulator of lifespan. Similar changes are seen in wild-type mice in response to chronic genotoxic stress, caloric restriction, or with ageing. We conclude that unrepaired cytotoxic DNA damage induces a highly conserved metabolic response mediated by the IGF1/insulin pathway, which re-allocates resources from growth to somatic preservation and life extension. This highlights a causal contribution of DNA damage to ageing and demonstrates that ageing and end-of-life fitness are determined both by stochastic damage, which is the cause of functional decline, and genetics, which determines the rates of damage accumulation and decline.

Numerous progeroid syndromes are caused by defects in the cellular response to DNA damage, including Cockayne syndrome, Werner syndrome, ataxia telangiectasia and trichothiodystrophy¹, suggesting that defective genome maintenance contributes to ageing. However, the value of progeroid syndromes for understanding normal human ageing is controversial²⁻⁴, primarily because symptoms are tissue-specific. The segmental nature of these progeroid syndromes is consistent with the disposable soma theory of ageing (which posits that ageing results from accumulated damage⁵), because damage is stochastic and each tissue has different requirements for the various repair mechanisms⁶. Nevertheless, the most consistent determinant of lifespan is the mitogenic growth hormone/IGF1 pathway^{7,8}. Prolonged dampening of the axis genetically or by caloric restriction promotes longevity, whereas persistent upregulation shortens life. Experimental evidence reconciling the apparently disparate mechanisms of progeroid syndromes and natural ageing is currently lacking.

Nucleotide excision repair (NER) is a multi-step 'cut and patch' mechanism that removes distorting lesions affecting one strand of DNA such as those resulting from ultraviolet (UV) radiation damage. Two subpathways exist: transcription-coupled NER (TC-NER) and global genome NER (GG-NER). TC-NER removes lesions that block RNA polymerases, rescuing transcription and preventing cell death. Defective TC-NER causes Cockayne syndrome and trichothiodystrophy⁹. GG-NER operates genome-wide, primarily preventing mutations. Defective GG-NER causes the cancer-prone syndrome

xeroderma pigmentosum⁹. Xeroderma pigmentosum patients (complementation groups XP-A to XP-G) have over a 1,000-fold increased risk of skin cancer and a 10-fold increased risk of other tumours⁹. The contrasting phenotypes of Cockayne syndrome, trichothiodystrophy and xeroderma pigmentosum suggest that the cellular response to DNA damage dictates outcome: cell death/senescence accelerates ageing whereas cell survival (with mutations) promotes cancer¹⁰.

XPF-ERCC1 is an endonuclease required for NER¹¹. XPF is catalytic¹² and ERCC1 is essential for DNA binding¹³. Uniquely, this complex is also required for DNA interstrand crosslink (ICL) repair¹⁴. ICLs link both strands of DNA, preventing transcription and replication, and hence are extremely cytotoxic. Remarkably, XP-F patients have mild xeroderma pigmentosum¹¹, residual repair and only subtle *XPF* mutations. No patients with mutations in *ERCC1* are reported. Because complete inactivation of GG-NER or TC-NER is compatible with life, this suggests that the additional functions of XPF-ERCC1, including ICL repair, are essential. Here we describe a progeroid syndrome caused by a severe mutation in *XPF* and evidence from a mouse model of the disease that the growth hormone/IGF1 hormonal axis, a known regulator of lifespan, is suppressed in response to cytotoxic DNA damage.

A progeroid syndrome due to mutation of *XPF*

A boy aged 15 presented with frequent sunburns and a unique combination of progeroid symptoms (Supplementary Fig. 1 and

¹Center for Biomedical Genetics Medical Genetic Center Department of Cell Biology and Genetics, and ²Department of Experimental Radiology, and ³Department of Clinical Genetics, Erasmus Medical Center, PO Box 1738 3000 DR Rotterdam, The Netherlands. ⁴University of Pittsburgh Cancer Institute, Department of Molecular Genetics and Biochemistry, University of Pittsburgh School of Medicine, 5117 Centre Avenue, Pittsburgh, Pennsylvania 15213, USA. ⁵Abteilung für Medizinische Genetik, Altonaer KinderKrankenhaus, Bleickenallee 38, 22763 Hamburg, Germany. ⁶The Buck Institute for Age Research, 8001 Redwood Boulevard, Novato, California 94945, USA.

Supplementary Information 1). Inborn photosensitivity is indicative of defective NER. Indeed, poor survival after UV irradiation, reduced UV-radiation-induced DNA repair synthesis and impaired RNA synthesis recovery after UV irradiation of the patient's fibroblasts (the XPF-ERCC1 (XFE) fibroblasts; Fig. 1a, b; Supplementary Fig. 2 and Supplementary Information 2 Methods) indicated an almost complete absence of GG-NER and TC-NER, characteristic of both xeroderma pigmentosum and Cockayne syndrome. However, the neurologic, hepatobiliary, musculoskeletal and haematopoietic symptoms clearly discriminate this syndrome from xeroderma pigmentosum, Cockayne syndrome or combined xeroderma pigmentosum-Cockayne syndrome. Complementation analysis indicated that XFE cells are defective in XPF (Supplementary Fig. 2). This was unanticipated: all XP-F patients have substantial residual NER and mild xeroderma pigmentosum^{15,16}. XFE complementary DNA revealed a G→C transversion at position 458 in *XPF*, predicting a non-conservative substitution of a highly conserved arginine (R153P) (Supplementary Fig. 2; GenBank Accession number NM_005236). The patient's genomic DNA demonstrated homozygosity for this mutation. R153 resides in a domain harbouring helicase motifs¹³ and a leucine-rich region frequently involved in protein interactions. XPF and ERCC1 levels were lower in XFE cells than cells from XP-F patients (Fig. 1c, d), but detectable. XFE fibroblasts were exquisitely sensitive to ICL damage (Fig. 1e), confirming a role for XPF-ERCC1 in ICL resistance, distinct from that in NER. The unique clinical and cellular parameters define a novel disorder that we term XFE progeroid syndrome.

Ercc1^{-/-} mice model XFE progeroid syndrome

In mice, ERCC1- and XPF-null mutants are viable¹⁷⁻¹⁹ (Supplementary Table 1), but their severe phenotype is quite distinct from NER deficiency²⁰. Embryonic and early post-natal development of

Ercc1^{-/-} mice is mildly retarded, but growth arrests dramatically in the second week, typically culminating in death by four weeks (Fig. 2a, b and Supplementary Fig. 3a, b). *Ercc1*^{-/-} mice show ageing-like skin, liver and bone marrow abnormalities^{17,18,21}. We additionally identified dystonia and progressive ataxia (both indicative of neurodegeneration), renal insufficiency, sarcopenia, kyphosis and, at the cellular level, premature replicative senescence and sensitivity to oxidative stress (Fig. 2c, d and Supplementary Figs 3c and 4)—all changes associated with advanced age.

Early postnatal development was normal in patient 'XFE'. The progeroid symptoms initiated in early prepubescence, resulted in death before sexual maturation and included an old, wizened appearance, weight loss, epidermal atrophy, visual and hearing loss, ataxia, cerebral atrophy, hypertension, liver dysfunction, anaemia, osteopaenia, kyphosis, sarcopaenia and renal insufficiency. There is a striking correlation between the human syndrome and the *Ercc1*^{-/-} mouse phenotype (Supplementary Table 2). Importantly, XPF is undetectable in *Ercc1*^{-/-} mouse tissue (Supplementary Fig. 3d), indicating destabilization of the complex²². Furthermore, like XFE,

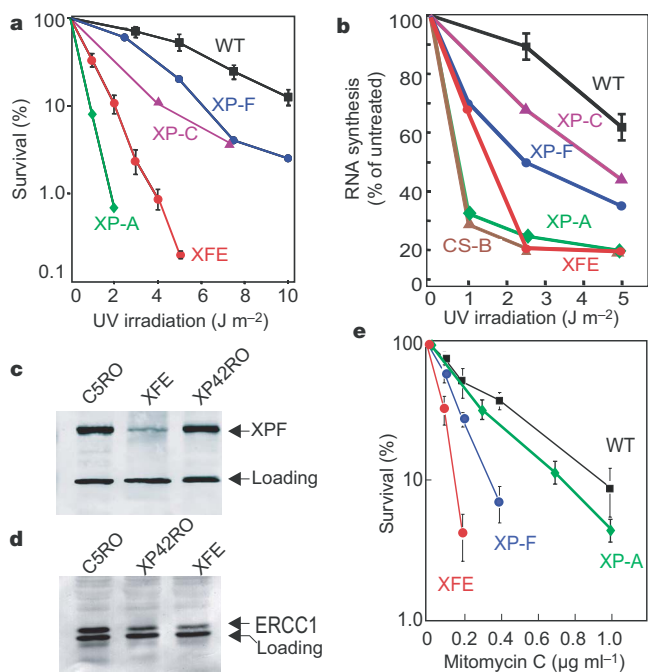


Figure 1 | Molecular characterization of progeroid patient 'XFE'.

a, Clonogenic survival assay measuring UV-radiation sensitivity of wild-type (WT), XFE and xeroderma pigmentosum patient primary fibroblasts (XP-F, XP-C and XP-A). **b**, RNA synthesis recovery after UV irradiation of patient fibroblasts. **c**, Immunodetection of XPF in nuclear extracts of patient fibroblasts (normal C5RO, mild xeroderma pigmentosum patient XP42RO and patient XFE). Cross-reacting bands demonstrate equal protein loading. **d**, Immunodetection of ERCC1 in the same samples. **e**, Clonogenic survival assay measuring sensitivity of patient fibroblasts to the crosslinking agent mitomycin C. Error bars (**a**, **b**, **e**) indicate s.e.m. of three experiments.

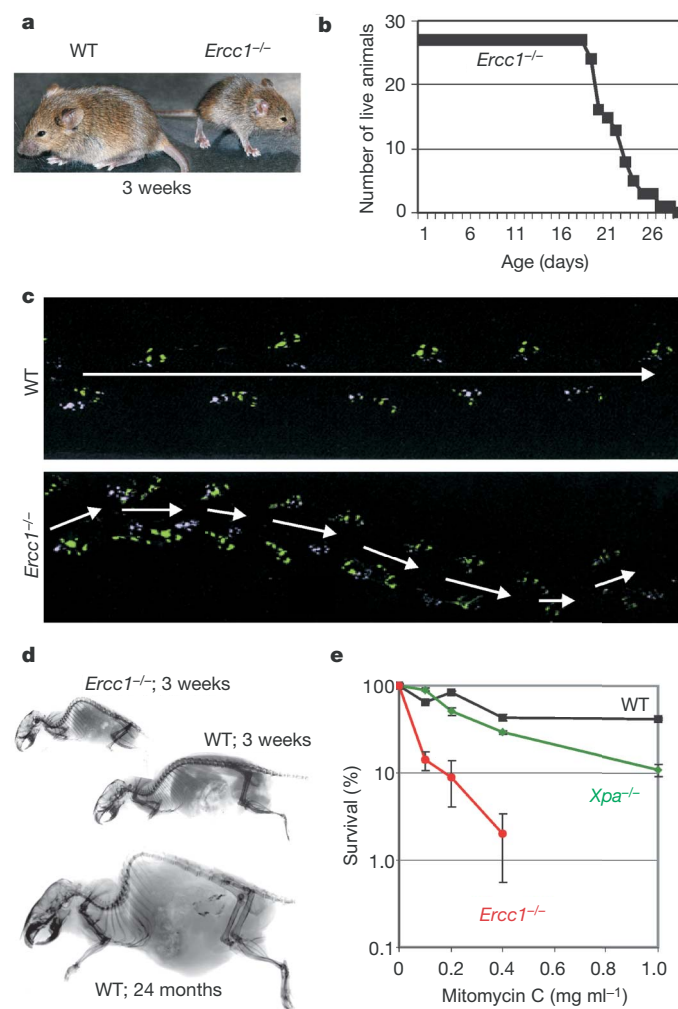


Figure 2 | Progeroid characteristics of *Ercc1*^{-/-} mice. **a**, *Ercc1*^{-/-} mouse and wild-type littermate at 3 weeks of age. **b**, Lifespan of *Ercc1*^{-/-} mice ($n = 27$). **c**, Footprint analysis of 3-week-old mice. Forepaws were painted purple, hind paws green. The arrows indicate gait trajectory. Fore- and hind-prints are not superimposed in mutant animals, a diagnostic criteria of ataxia. **d**, Radiographs demonstrating kyphosis in an aged wild-type and in an *Ercc1*^{-/-} mouse, but not in a young wild-type mouse. **e**, Clonogenic survival assay measuring the sensitivity of primary mouse embryonic fibroblasts to the crosslinking agent mitomycin C. Error bars indicate s.e.m. for three experiments, each averaging three replica platings of cells.

Ercc1^{-/-} cells are more sensitive to ICL damage than other NER-deficient cells (Fig. 2e). Collectively, these data establish *Ercc1*^{-/-} mice as an accurate model of the XFE progeroid syndrome.

Expression changes in *Ercc1*^{-/-} mouse liver

To investigate the cause of the progeroid features, we compared the entire transcriptome of *Ercc1*^{-/-} mouse liver with that of wild-type littermates at the age of 15 days, when the *Ercc1*^{-/-} mice reached maximal weight (Supplementary Fig. 3b), and had progeroid symptoms but only limited pathology. The liver was selected because it showed well-defined ageing-related changes and evidence for genotoxic stress (stabilized p53)¹⁷. Two-tailed, *t*-test analysis of variance of Affymetrix full genome arrays revealed 1,675 genes with significantly changed expression in *Ercc1*^{-/-} compared with wild-type liver ($\geq \pm 1.2$ -fold change and $P \leq 0.01$; Supplementary Table 3). Gene ontology classification (Supplementary Table 4) revealed: (1) global attenuation of the somatotroph, lactotroph and thyrotroph hormonal axes and other growth-promoting mechanisms; (2) downregulation of oxidative and carbohydrate metabolism; (3) upregulation of genes associated with glycogen synthesis but downregulation of glycogen phosphorylase, indicating a propensity to store not use glucose, an anticipated response to hyposomatotropism; (4) upregulation of fatty acid synthesis, the leptin receptor (*Lepr*) and peroxisome proliferator-activated receptor (*Ppar*)- γ and $-\alpha$, further suggesting an attempt to store energy; (5) upregulation of anti-oxidant and detoxification defences; (6) upregulation of DNA repair, suggesting increased damage load; and (7) upregulation of pro-apoptotic genes and downregulation of anti-apoptotic genes, indicating spontaneous hepatocellular toxicity. Remarkably, the majority of these metabolic changes are associated with extended lifespan in *Caenorhabditis elegans*²³.

Quantitative real-time PCR (qRT-PCR) of key genes in the pathways confirmed these findings in the liver, extended them to the kidney, and identified a trend towards increasing changes in expression with age (Fig. 3a, b), indicating a systemic, progressive process. The predicted downregulation of the growth hormone/IGF1 somatotroph axis in *Ercc1*^{-/-} mice explains their post-natal growth retardation. IGF1 is synthesized and secreted by the liver in response to growth hormone and is primarily responsible for its growth-promoting effects²⁴; thus it is a terminal read-out of the somatotroph axis. Circulating IGF1 levels in *Ercc1*^{-/-} mice were significantly lower than wild-type littermates (Fig. 3c; $P < 0.001$). These data predict a state of glucose storage rather than usage in *Ercc1*^{-/-} mice. In accordance, blood glucose levels were significantly lower than control littermates (Fig. 3d; $P < 0.001$). *Ercc1*^{-/-} mice were also hypoinsulinaemic (Fig. 3e; $P < 0.03$), consistent with insulin sensitivity and

elevated expression of *Ppar*- γ . These data validate the metabolic changes predicted by microarray analysis.

Suppression of the growth hormone axis in response to DNA damage

A primary defect in the hypothalamus or pituitary gland is not the cause of low IGF1 in *Ercc1*^{-/-} mice: immunohistochemistry of the anterior pituitary (which contains somatotrophs) revealed no pathology, normal numbers of growth-hormone-positive cells (Fig. 4a), and viable somatotrophs (Fig. 4b). Moreover, serum growth hormone of *Ercc1*^{-/-} mice was within the normal range (Fig. 4c) or tended to be elevated, as expected in response to low IGF1 and growth hormone receptor through feedback regulatory mechanisms. This raises the possibility that reduced IGF1 represents an adaptive response to DNA damage. Interestingly, chronic exposure of adult wild-type mice to subtoxic doses of the crosslinking agent mitomycin C suppressed serum IGF1 (Fig. 4d). In addition, qRT-PCR data indicated similar expression changes in the liver of mitomycin-C-exposed mice as seen in *Ercc1*^{-/-} mice (Supplementary Fig. 5). These results demonstrate that the systemic response in *Ercc1*^{-/-} mice, resulting from their DNA repair defect, is elicited in normal organisms that are challenged with genotoxic stress.

Parallels between XPF-ERCC1 deficiency and ageing

The somatotroph axis declines with age in mammals, including man^{8,25}. This prompted us to systematically compare broader expression changes in *Ercc1*^{-/-} and aged mice. The complete liver transcriptomes of 16-week-old and 130-week-old wild-type mice were compared with that of 8-week-old wild-type mice to identify expression changes in young adult (16 weeks) and aged (130 weeks) mice relative to juveniles (8 weeks) (Supplementary Table 5–7). Gene ontology classification of these gene sets indicated global suppression of the somatotroph axis, carbohydrate and oxidative metabolism, peroxisome biogenesis and ATP synthesis, but upregulation of immune and inflammatory responses and protein glycosylation in aged, but not young adult mice, concurring with previous studies in aged murine skeletal muscle and liver^{26,27}. Biological pathways that were similarly affected in *Ercc1*^{-/-} and aged wild-type mice included: the somatotroph axis, carbohydrate and oxidative metabolism, and peroxisome biogenesis. Apoptotic and anti-oxidant responses were largely unique to *Ercc1*^{-/-} mice, whereas inflammatory responses and protein glycosylation were unique to aged mice.

To quantify the similarity between *Ercc1*^{-/-} and aged mice, we asked how many of the 1,675 differentially expressed genes in the *Ercc1*^{-/-} liver transcriptome were altered in the same direction in aged mice? A 100% correlation yields a Spearman rank correlation

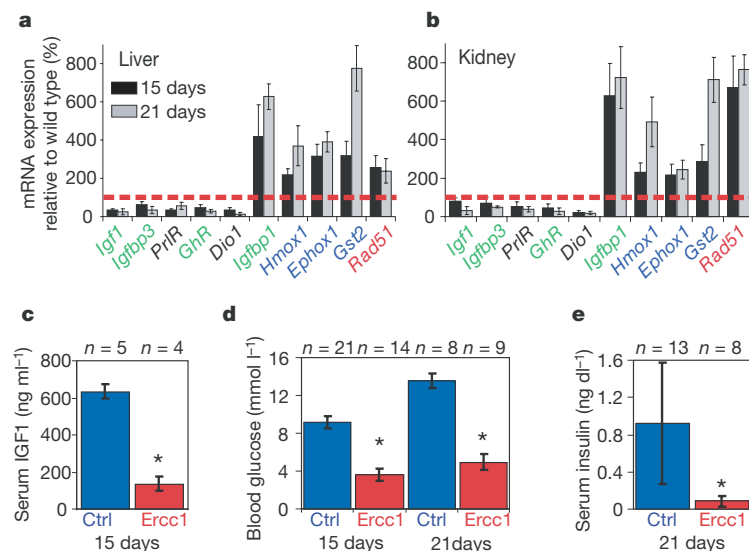


Figure 3 | Confirmation of microarray expression data by qRT-PCR and physiologic endpoints. **a**, qRT-PCR of liver messenger RNA levels of genes associated with the growth hormone/IGF1 axis (green), other hormonal axes (black), oxidant defence (blue), and DNA repair (red) in the liver of 15-day-old (black) and 21-day-old (grey) *Ercc1*^{-/-} mice relative to wild-type-littermates (red line). Each bar represents the average of three animals \pm s.d. **b**, Similar analysis on the kidney. **c**, Serum IGF1 levels in *Ercc1*^{-/-} mice and littermate controls (Ctrl). Average values for 4–5 animals are plotted \pm s.e.m. (* $P < 0.001$). **d**, Blood glucose levels of 15-day-old and 21-day-old *Ercc1*^{-/-} mice and control littermates. Average values for 8–21 animals are plotted \pm s.e.m. (* $P < 0.001$). **e**, Serum insulin levels of 3-week-old *Ercc1*^{-/-} mice and control littermates. Average values for 8–13 animals are plotted \pm s.e.m. (* $P < 0.03$).

coefficient ρ (r) of 1.0. The expression pattern of *Ercc1*^{-/-} mice had a significant degree of correlation with old mice ($r = 0.32$, $P \leq 0.0001$), but not young mice ($r = -0.03$). When the comparison was restricted to those biological themes that were significantly over-represented in the *Ercc1*^{-/-} mouse liver, there was an 86% correlation and within the somatotroph axis 95% (Supplementary Table 8). Therefore, despite the tremendous difference in age and genetic background, the transcriptional changes in *Ercc1*^{-/-} mice and old mice showed a highly significant correlation. Importantly, the liver transcriptomes of *Xpa*^{-/-} (nullizygous for the essential NER protein XPA) and *Csb*^{m/m} mice (homozygous for a mutation in *Csb* that leads to Cockayne syndrome), which are NER-deficient but not progeroid, did not significantly overlap with that of old mice, but the transcriptome of severely progeroid *Xpa*^{-/-};*Csb*^{m/m} mice did ($r = 0.44$; $P \leq 0.0001$)²⁸. Thus, we identified a common pattern of gene expression changes between aged and progeroid DNA-repair-deficient mice.

Cellular proliferation was drastically decreased in both *Ercc1*^{-/-} and aged mice (Fig. 5a), as predicted by microarray analysis. Further, senescent, polyploid hepatocytes, a hallmark of ageing²⁹, were prominent in both the *Ercc1*^{-/-} and aged mice, but not immature animals (Fig. 5a). Apoptotic cells were dramatically increased in *Ercc1*^{-/-} mouse liver and to a lesser extent in aged mice (Fig. 5b). Lysochrome staining revealed triglyceride accumulation in the liver of *Ercc1*^{-/-} and aged mice, which is consistent with decreased oxidative

metabolism (Fig. 5c). Steatosis was more pronounced in 21- than 15-day-old *Ercc1*^{-/-} mice, indicating a progressive process. Finally, IGFBP1—a protein overexpressed in response to liver injury, fasting or hypoinsulinemia³⁰—was extremely elevated in *Ercc1*^{-/-} and aged-mouse liver compared with that of young wild-type mice (Fig. 5d). These data confirm that the diverse metabolic changes predicted by expression analysis are similarly altered in *Ercc1*^{-/-} and aged mice.

A model connecting DNA damage, the growth hormone axis and ageing

Different mutations in *XPF* result in distinct clinical outcomes: either cancer as in xeroderma pigmentosum, or progeroid symptoms as in XFE syndrome. One explanation is that the R153 XFE mutation, compromising both NER and ICL repair, results primarily in cell death and senescence in response to DNA damage. This suppresses carcinogenesis^{31,32} but enhances ageing^{33–35}. In contrast, the milder NER defect in classic XP-F patients causes less cell death, allowing mutation accumulation and consequently cancer (elaborated in Supplementary Information 3). The specific sensitivity of XPF-ERCC1-deficient cells to crosslink damage, make ICLs a likely candidate for contributing to the unique phenotype of the XFE progeroid syndrome. Although spontaneous ICLs escape detection by current technology, several abundant endogenous compounds, many of which are by-products of lipid peroxidation, are known to crosslink DNA^{36,37}. Intriguingly, IGFBP1, which is extremely elevated in the *Ercc1*^{-/-} mouse liver (Fig. 5d), is strongly induced in rodents exposed to the crosslinking agent cisplatin³⁸ or fed a diet rich in polyunsaturated fatty acids³⁹, which promotes lipid peroxidation⁴⁰. Our data indicate that accumulation of nuclear DNA damage causes many of the pathophysiologic and metabolic changes associated with ageing, probably through increased cell death or senescence, without mutations and telomere loss^{41,42}. This is consistent with the damage accumulation theory of ageing^{6,43} and predicts that cytotoxic genotoxins used in adjuvant chemotherapy for cancer may promote ageing⁴⁴.

A key observation was that the somatotroph axis is suppressed when DNA damage is increased either genetically or chemically. This result is consistent with the observation that genetic deletion of SIRT6, a protein ADP ribosyl-transferase that positively affects lifespan and genome integrity, also suppresses IGF1⁴⁵. In addition, overexpression of the short isoform of p53 in mice impairs genome maintenance and IGF1 signalling³⁴. Together these studies create an inexorable link between genome maintenance and the somatotroph axis.

Direct genetic disruption of the growth hormone axis in mice leads to metabolic changes, including low serum glucose and insulin, improved insulin sensitivity, increased expression of *Ppar-γ*, decreased β -oxidation of fatty acids, increased gluconeogenesis, and enhanced anti-oxidant defenses and stress resistance⁶. As a consequence, these mice have reduced growth, body weight and fertility, yet increased lifespan and delayed onset of age-associated morbidities⁸. Caloric restriction causes rapid and reversible transcriptional reprogramming resulting in decreased insulin/IGF1 signalling with similar downstream effects⁴⁶. Our data indicate a near-identical pattern of metabolic and growth changes in *Ercc1*^{-/-} mice. This supports the existence of a common stress response, mediated by the insulin pathway, providing self-protection in the face of diverse stressors—a phenomenon termed hormesis, with reference to caloric restriction⁴⁷.

Multiple types of cellular and molecular damage accumulate with age⁶, and could trigger the same stress response. This likelihood is supported by the highly significant correlation between the transcriptomes of *Ercc1*^{-/-} mice and old mice, as well as the fact that growth hormone/IGF1 signalling decreases with age in mammals⁴⁸. On this basis, we propose the following model to explain how DNA damage (and probably other types of molecular damage) contributes to ageing (Fig. 5e). Damage accumulates with time as a consequence of exposure to endogenous and environmental genotoxins and incomplete repair. The DNA damage triggers a stress response either

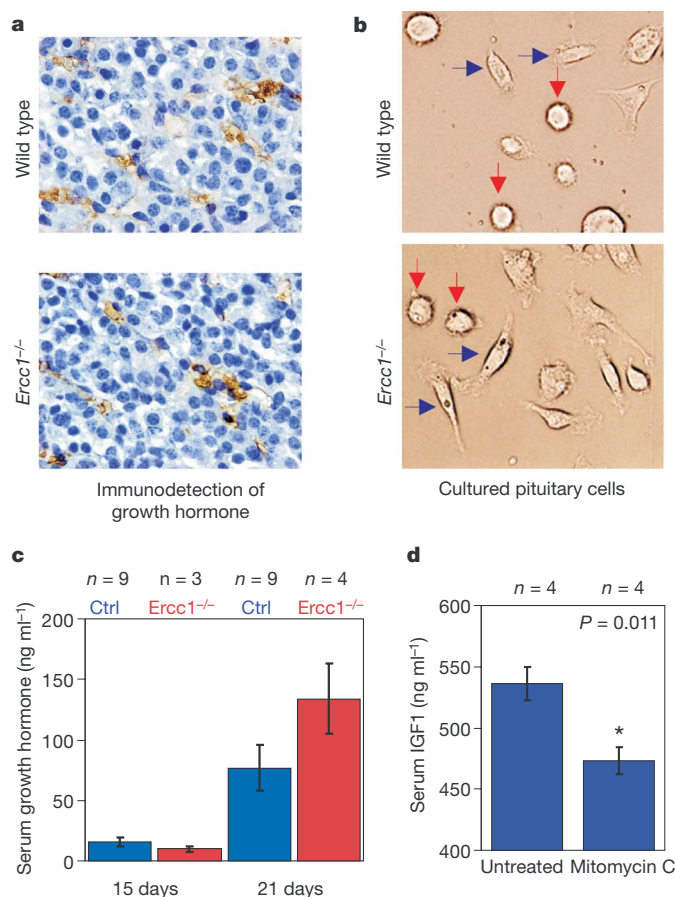


Figure 4 | Growth-hormone-IGF1 suppression is a normal physiological response to DNA damage. **a**, Immunodetection of growth hormone (brown) in anterior pituitary of wild-type and *Ercc1*^{-/-} mice. **b**, Cultured cells from the pituitary of wild-type and *Ercc1*^{-/-} mice indicating a normal distribution and viability of somatotrophs (blue arrows) and lactotrophs (red arrows). **c**, Serum growth hormone levels of 15- and 21-day-old *Ercc1*^{-/-} mice (red) and littermate controls (blue) (non-significant; $P = 0.4$, 15 days; $P = 0.12$, 21 days). **d**, Serum IGF1 levels of adult wild-type mice chronically exposed to mitomycin C (0.1 mg kg⁻¹ bimonthly) compared with untreated mice ($n = 4$ per group; $*P = 0.011$). Error bars, s.e.m.

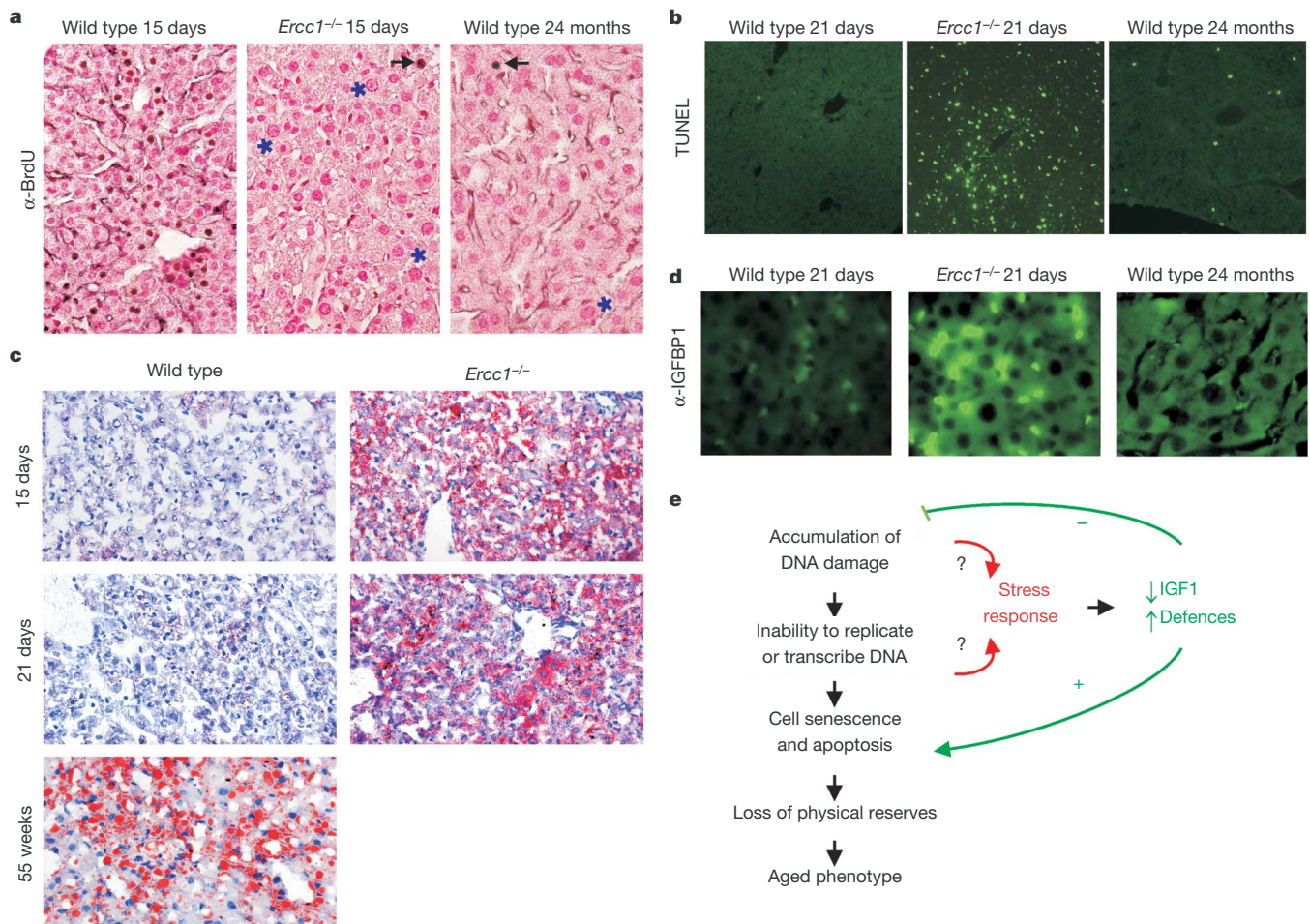


Figure 5 | Comparison of the physiological changes due to DNA repair defects and ageing. **a**, Detection of proliferating cells in liver of *Ercc1*^{-/-}, young and old wild-type mice by immunodetection of incorporated BrdU (brown nuclei and arrows). Large, polyploidy nuclei are apparent in the

Ercc1^{-/-} and aged mouse liver (asterisks). **b**, Measurement of apoptotic nuclei in liver by TUNEL assay. **c**, Detection of triglycerides in liver with the lysochrome Oil Red O. **d**, Immunodetection of IGFBP1 in the liver. **e**, Model of how DNA damage contributes to ageing (see text for details).

directly or by interfering with transcription or replication. The response is systemic dampening of the growth hormone/IGF1 hormonal axis, through a mechanism that is, as yet, unknown, but is highly conserved⁶⁻⁸. This in turn leads to metabolic changes that shift energy usage from growth and proliferation to protective maintenance⁷, minimizing further damage, but contributing to apoptosis⁴⁹. Despite this protective response, organisms which continue to accumulate damage will inevitably age. Repair-deficient *Ercc1*^{-/-} mice continue to rapidly accumulate DNA damage and experience an early onset of degenerative processes. Aged organisms in which either damage prevention or repair mechanisms may already be compromised will continue to accumulate damage slowly, eventually succumbing to age-related morbidities and mortality. In both examples, the 'ageing process' is retarded by the insulin-mediated stress response.

This model reconciles two apparently disparate hypotheses of ageing: that ageing is genetically regulated⁷ and that ageing is a consequence of the accumulation of stochastic damage⁶. In fact, both are correct. Damage drives the functional decline that is associated with ageing; however, a highly conserved longevity assurance mechanism, mediated by the IGF1/insulin pathway, influences how rapidly damage accumulates and function is lost.

METHODS

Detailed methods are provided in Supplementary Information 2. Cell lines were established from skin biopsies of patients or from mouse embryos. Nucleotide excision repair was measured by a clonogenic survival assay after exposure of

cells to UV irradiation (UV-C, 254 nm). Unscheduled DNA synthesis (a measure of GG-NER) was determined by quantifying incorporation of ³H-thymidine into genomic DNA after exposure of cells to 10 J m⁻² of UV-C radiation. RNA synthesis recovery (TC-NER) was measured as ³H-uridine incorporation after UV irradiation of cells. *XPF* was identified as the gene affected in patient XFE by fusing his cells with those of a patient from each complementation group of xeroderma pigmentosum and measuring unscheduled DNA synthesis. Both *XPF* cDNA and exons from gDNA isolated from XFE cells were sequenced. Crosslink sensitivity was determined by clonogenic survival assay following exposure to mitomycin C. Antibodies and ELISA kits used for immunodetection of XPF, ERCC1, IGF1, insulin, glucose, growth hormone, BrdU incorporation and IGFBP1; tissue staining; and TUNEL (TdT-mediated dUTP nick end labelling) reagents are elaborated in Supplementary Information 2.

Ercc1^{-/-} mice were generated in an F₁ hybrid background by crossing *Ercc1*^{+/-} mice. Genomic DNA was isolated from an ear punch and genotyped by PCR. Ataxia in mice was measured by analysing gait after painting fore- and hind-paws with different colours. X-rays were obtained with a CGR Senograph 500T instrument. Genome-wide expression profiles were determined for liver of 15-day-old *Ercc1*^{-/-} mice and wild-type littermates, as well as 8-, 16- and 130-week-old C57BL/6J mice using Affymetrix 430 V2.0 arrays. Expression changes were confirmed by qRT-PCR for 16 genes representing each of the biological themes significantly affected in *Ercc1*^{-/-} and aged mice. For chronic genotoxin exposure studies, adult wild-type mice (10 weeks old; *n* = 4) were administered 0.1 mg kg⁻¹ mitomycin C bimonthly for 10 weeks.

Received 11 September; accepted 20 November 2006.

- Hasty, P., Campisi, J., Hoeijmakers, J., van Steeg, H. & Vijg, J. Aging and genome maintenance: lessons from the mouse? *Science* 299, 1355-1359 (2003).
- Kipling, D., Davis, T., Ostler, E. L. & Faragher, R. G. What can progeroid syndromes tell us about human aging? *Science* 305, 1426-1431 (2004).

3. Hasty, P. & Vijg, J. Accelerating aging by mouse reverse genetics: a rational approach to understanding longevity. *Aging Cell* **3**, 55–65 (2004).
4. Miller, R. A. Evaluating evidence for aging. *Science* **310**, 441–443; author reply 441–443 (2005).
5. Kirkwood, T. B. & Holliday, R. The evolution of ageing and longevity. *Proc. R. Soc. Lond. B* **205**, 531–546 (1979).
6. Kirkwood, T. B. Understanding the odd science of aging. *Cell* **120**, 437–447 (2005).
7. Kenyon, C. The plasticity of aging: insights from long-lived mutants. *Cell* **120**, 449–460 (2005).
8. Bartke, A. Minireview: role of the growth hormone/insulin-like growth factor system in mammalian aging. *Endocrinology* **146**, 3718–3723 (2005).
9. Bootsma, D., Kraemer, K. H., Cleaver, J. E. & Hoeijmakers, J. H. J. in *The Metabolic and Molecular Basis of Inherited Disease* (eds Scriver, C. R. et al.) 677–703 (McGraw-Hill, New York, 2001).
10. Mitchell, J. R., Hoeijmakers, J. H. & Niedernhofer, L. J. Divide and conquer: nucleotide excision repair battles cancer and ageing. *Curr. Opin. Cell Biol.* **15**, 232–240 (2003).
11. Sijbers, A. M. et al. Xeroderma pigmentosum group F caused by a defect in a structure-specific DNA repair endonuclease. *Cell* **86**, 811–822 (1996).
12. Enzlin, J. H. & Scharer, O. D. The active site of the DNA repair endonuclease XPF-ERCC1 forms a highly conserved nuclease motif. *EMBO J.* **21**, 2045–2053 (2002).
13. Tsodikov, O. V., Enzlin, J. H., Scharer, O. D. & Ellenberger, T. Crystal structure and DNA binding functions of ERCC1, a subunit of the DNA structure-specific endonuclease XPF-ERCC1. *Proc. Natl Acad. Sci. USA* **102**, 11236–11241 (2005).
14. Niedernhofer, L. J. et al. The structure-specific endonuclease Ercc1-Xpf is required to resolve DNA interstrand cross-link-induced double-strand breaks. *Mol. Cell Biol.* **24**, 5776–5787 (2004).
15. Matsumura, Y., Nishigori, C., Yagi, T., Imamura, S. & Takebe, H. Characterization of molecular defects in xeroderma pigmentosum group F in relation to its clinically mild symptoms. *Hum. Mol. Genet.* **7**, 969–974 (1998).
16. Sijbers, A. M. et al. Homozygous R788W point mutation in the XPF gene of a patient with xeroderma pigmentosum and late-onset neurologic disease. *J. Invest. Dermatol.* **110**, 832–836 (1998).
17. McWhir, J., Selfridge, J., Harrison, D. J., Squires, S. & Melton, D. W. Mice with DNA repair gene (ERCC-1) deficiency have elevated levels of p53, liver nuclear abnormalities and die before weaning. *Nature Genet.* **5**, 217–224 (1993).
18. Weeda, G. et al. Disruption of mouse ERCC1 results in a novel repair syndrome with growth failure, nuclear abnormalities and senescence. *Curr. Biol.* **7**, 427–439 (1997).
19. Tian, M., Shinkura, R., Shinkura, N. & Alt, F. W. Growth retardation, early death, and DNA repair defects in mice deficient for the nucleotide excision repair enzyme XPF. *Mol. Cell Biol.* **24**, 1200–1205 (2004).
20. de Vries, A. et al. Increased susceptibility to ultraviolet-B and carcinogens of mice lacking the DNA excision repair gene XPA. *Nature* **377**, 169–173 (1995).
21. Prasher, J. M. et al. Reduced hematopoietic reserves in DNA interstrand crosslink repair-deficient Ercc1^{-/-} mice. *EMBO J.* **24**, 861–871 (2005).
22. Biggerstaff, M., Szymkowski, D. E. & Wood, R. D. Co-correction of the ERCC1, ERCC4 and xeroderma pigmentosum group F DNA repair defects *in vitro*. *EMBO J.* **12**, 3685–3692 (1993).
23. Hansen, M., Hsu, A. L., Dillin, A. & Kenyon, C. New genes tied to endocrine, metabolic, and dietary regulation of lifespan from a *Caenorhabditis elegans* genomic RNAi screen. *PLoS Genet.* **1**, 119–128 (2005).
24. Carter, C. S., Ramsey, M. M. & Sonntag, W. E. A critical analysis of the role of growth hormone and IGF-1 in aging and lifespan. *Trends Genet.* **18**, 295–301 (2002).
25. Lombardi, G., Di Somma, C., Rota, F. & Colao, A. Associated hormonal decline in aging: is there a role for GH therapy in aging men? *J. Endocrinol. Invest.* **28**, 99–108 (2005).
26. Lee, C. K., Klopp, R. G., Weindruch, R. & Prolla, T. A. Gene expression profile of aging and its retardation by caloric restriction. *Science* **285**, 1390–1393 (1999).
27. Cao, S. X., Dhahbi, J. M., Mote, P. L. & Spindler, S. R. Genomic profiling of short- and long-term caloric restriction effects in the liver of aging mice. *Proc. Natl Acad. Sci. USA* **98**, 10630–10635 (2001).
28. van der Pluijm, I. et al. Impaired genome maintenance suppresses the GH/IGF1 axis in Cockayne syndrome mice. *PLoS Biol.* doi:10.1371/journal.pbio.0050002 (in the press).
29. Gupta, S. Hepatic polyploidy and liver growth control. *Semin. Cancer Biol.* **10**, 161–171 (2000).
30. Lee, P. D., Conover, C. A. & Powell, D. R. Regulation and function of insulin-like growth factor-binding protein-1. *Proc. Soc. Exp. Biol. Med.* **204**, 4–29 (1993).
31. Campisi, J. Aging, tumor suppression and cancer: high wire-act! *Mech. Ageing Dev.* **126**, 51–58 (2005).
32. Sonntag, W. E. et al. Adult-onset growth hormone and insulin-like growth factor I deficiency reduces neoplastic disease, modifies age-related pathology, and increases life span. *Endocrinology* **146**, 2920–2932 (2005).
33. Wyllie, F. S. et al. Telomerase prevents the accelerated cell ageing of Werner syndrome fibroblasts. *Nature Genet.* **24**, 16–17 (2000).
34. Maier, B. et al. Modulation of mammalian life span by the short isoform of p53. *Genes Dev.* **18**, 306–319 (2004).
35. Herbig, U., Ferreira, M., Condel, L., Carey, D. & Sedivy, J. M. Cellular senescence in aging primates. *Science* **311**, 1257 (2006).
36. Kasai, H., Iwamoto-Tanaka, N. & Fukada, S. DNA modifications by the mutagen glyoxal: adduction to G and C, deamination of C and GC and GA cross-linking. *Carcinogenesis* **19**, 1459–1465 (1998).
37. Niedernhofer, L. J., Daniels, J. S., Rouzer, C. A., Greene, R. E. & Marnett, L. J. Malondialdehyde, a product of lipid peroxidation, is mutagenic in human cells. *J. Biol. Chem.* **278**, 31426–31433 (2003).
38. Huang, Q. et al. Assessment of cisplatin-induced nephrotoxicity by microarray technology. *Toxicol. Sci.* **63**, 196–207 (2001).
39. Ghoshal, A. K., Xu, Z., Wood, G. A. & Archer, M. C. Induction of hepatic insulin-like growth factor binding protein-1 (IGFBP-1) in rats by dietary n-6 polyunsaturated fatty acids. *Proc. Soc. Exp. Biol. Med.* **225**, 128–135 (2000).
40. Takahashi, Y., Kushiro, M., Shinohara, K. & Ide, T. Activity and mRNA levels of enzymes involved in hepatic fatty acid synthesis and oxidation in mice fed conjugated linoleic acid. *Biochim. Biophys. Acta* **1631**, 265–273 (2003).
41. Zhu, X. D. et al. ERCC1/XPF removes the 3' overhang from uncapped telomeres and represses formation of telomeric DNA-containing double minute chromosomes. *Mol. Cell* **12**, 1489–1498 (2003).
42. Dollé, M. E. et al. Increased genomic instability is not a prerequisite for shortened lifespan in DNA repair deficient mice. *Mutat. Res.* **596**, 22–35 (2006).
43. Lombard, D. B. et al. DNA repair, genome stability, and aging. *Cell* **120**, 497–512 (2005).
44. McCormick, R. E. Possible acceleration of aging by adjuvant chemotherapy: a cause of early onset frailty? *Med. Hypotheses* **67**, 212–215 (2006).
45. Mostoslavsky, R. et al. Genomic instability and aging-like phenotype in the absence of mammalian SIRT6. *Cell* **124**, 315–329 (2006).
46. Spindler, S. R. Rapid and reversible induction of the longevity, anticancer and genomic effects of caloric restriction. *Mech. Ageing Dev.* **126**, 960–966 (2005).
47. Kirkwood, T. B. & Shanley, D. P. Caloric restriction, hormesis and life history plasticity. *Hum. Exp. Toxicol.* **19**, 338–339 (2000).
48. Muller, E. E., Locatelli, V. & Cocchi, D. Neuroendocrine control of growth hormone secretion. *Physiol. Rev.* **79**, 511–607 (1999).
49. Pinkston, J. M., Garigan, D., Hansen, M. & Kenyon, C. Mutations that increase the life span of *C. elegans* inhibit tumor growth. *Science* **313**, 971–975 (2006).

Supplementary Information is linked to the online version of the paper at www.nature.com/nature.

Acknowledgements This research was supported by the National Institute of Aging Program, the Dutch Cancer Society, the Dutch Science Foundation (NWO) through the foundation of the Research Institute Diseases of the Elderly, as well as grants from SenterNovem IOP-Genomics, the NIH, the NIA Program Project, the NIEHS center, the EC, and Human Frontier Science Program. J.H.J.H. is chief scientific officer of DNAge. L.J.N. was supported by a postdoctoral fellowship from the American Cancer Society and subsequently by the NCI and The Ellison Medical Foundation, along with A.R.R. and A.A. We thank P. Nair, F. J. Calderon, R. B. Calder and D. Muñoz-Medellin of the Sam and Ann Barshop Center, University of Texas Health Science Center, for their contributions to the preliminary microarray analysis.

Author Contributions Human cells characterized by L.J.N., A.R., E.A., H.O., A.A., A.F.T., W.V. and N.G.J.J. Experimental analysis of mice by L.J.N., A.S.L., A.R.R. and R.O. Microarray analysis by L.J.N., G.A.G., G.T.J. v. d. H. and J.V. Radiography by W. v. L. Clinical services by P.M. and W.J.K. Manuscript prepared by L.J.N., G.A.G. and J.H.J.H.

Author Information The expression data for *Ercc1*^{-/-} mice are deposited in ArrayExpress (<http://www.ebi.ac.uk/arrayexpress/>), a public repository for microarray data, which stores Minimum Information for Microarray Experiments (MIAME)-compliant data in accordance with Microarray Gene Expression Data (MGED) recommendations. The accession number is E-MEXP-834. The accession number for the expression data on the aged mice is E-MEXP-839 (ref. 28). Reprints and permissions information is available at www.nature.com/reprints. The authors declare no competing financial interests. Correspondence and requests for materials should be addressed to J.H.J.H. (j.hoeijmakers@erasmusmc.nl).